ELSEVIER

Journal of Alloys and Compounds 217 (1995) 164–166

Journal of
ALLOYS
AND COMPOUNDS

On new Mo_2FeB_2-type representatives Ln_2Pt_2In

F. Hulliger

Laboratorium für Festkörperphysik ETH, CH-8093 Zürich, Switzerland

Received 1 June 1994

Abstract

Rare-earth compounds with compositions near Ln_2Pt_2In (Ln = La...Nd, Sm, Gd...Ho,) were found to crystallize in the tetragonal Mo_2FeB_2 structure, tP10, space group *P4/mbm* (no. 127), an ordered derivative of the U_3Si_2 structure. Among these, antiferromagnets and ferromagnets with ordering temperatures between 9 and 40 K were met.

Keywords: Lanthanide intermetallics; Ferromagnetism; Antiferromagnetism

Recently we reported [1] on the Mo_2FeB_2-type series Ln_2Pd_2In, which comprises all trivalent rare-earth elements Ln, as well as the actinides Th, U [2] and Np [2] and which probably could be extended to include trivalent actinides like Pu, Cm, Bk, Cf and so on. The tetragonal Mo_2FeB_2 structure, space group *P4/mbm* (no. 127), an ordered version of the U_3Si_2 type, is a fairly simple structure, so that the physical properties of its members are accessible to theoretical interpretations. The binary prototype occurs with minority elements of rather different character, such as Cr_3Si_2, Hf_3Ge_2, Nb_3B_2, Th_3Al_2, Ta_3Ga_2, Ta_3Be_2, Ca_3Hg_2, Eu_3Ag_2 and Gd_3Pd_2 [3]. Ternaries of rather unexpected composition are $LiNd_2Si_2$ and LiY_2Si_2 [4]. The atomic positions are shown in Table 1, where always $x_{4h} > 1/2 - x_{4g}$.

It is a strictly three-dimensional structure, although it can be generated from dumb-bell layers at $z = 0$ and $z = 1/2$ (for an illustration see Ref. [2]). The fourfold symmetry around the c-axis gives rise to a pattern of diamonds around squares or vice versa. The layer at $z = 0$ with the smaller dumb-bells contains an additional large atom at the centre of the squares. In three dimensions the squares are the equatorial sections of all-capped trigonal prismatic coordination polyhedra combined with double prisms. The discrete dumb-bell character would vanish if x_{Ln} or $(1/2 - x_T)$ approached $(\sqrt{3} - 1)/4 = 0.183$. For these values the distance between neighbours along the four square edges equals that within the dumb-bells. This does not occur in the representatives known until now. However, several examples exist where the length of the c-axis is similar to or even smaller than the distance within the dumb-bells of the larger elements (e.g. in U_2Co_2In, U_2Rh_2In, Np_2Pt_2In, U_2Ni_2In, U_2Pd_2In [2], U_2Fe_2Sn and U_2Rh_2Sn [5], which implies $x_{4h} > 8^{-1/2}(c/a)$ (e.g. for Ho_2Pt_2In this would require $x_{Ho} > 0.1686$). In these cases chains along the fourfold axis exist, which are of importance for magnetic interactions when the elements in 4h positions carry a magnetic moment or for superconductivity with d-elements.

Table 1
Atomic positions

U_3Si_2	Mo_2FeB_2	Ln_2T_2In				
U	Fe	In	2a	$x = 0$	$y = 0$	$z = 0$
Si	B	T	4g	$x \approx 0.37$–0.39	$y = 1/2 + x$	$z = 0$
U	Mo	Ln	4h	$x \approx 0.17$–0.18	$y = 1/2 + x$	$z = 1/2$

Up to now, unfortunately, we have found in our samples no single-crystal fragments appropriate for a structure determination, so that our structure assignment is based on intensity calculations with LAZY PULVERIX [6] and average atomic parameters [3].

We had no problems in synthesizing the Ln_2Pd_2In series [1]. Since Pd and Pt differ only marginally in size one might expect the Pt series to exist with all rare-earth elements. The Ln_2Pt_2In members with large Ln indeed formed without problems on reacting the elements in an argon arc. From erbium to lutetium the Ln_2Pt_2In phases possibly form peritectically. In the case of Er_2Pt_2In, annealing several weeks at 700 °C

SSDI 0925-8388(94)01357-8

was not sufficient to produce mainly the tetragonal phase. On the X-ray pattern the first and the strongest diffraction lines were faintly recognizable, but insufficient for reliable indexing. It appears that the electronegativities of Pd and Pt differ enough to cause the different behaviour. The difference is evident also in the binaries: Gd_3Pd_2...Tm_3Pd_2, for example, crystallize in the U_3Si_2 structure, whereas this phase is unknown for the corresponding Ln_3Pt_2 compounds. On the other hand, the platinides Ln_3Pt_2, with Ln = La...Nd, crystallize in the rhombohedral Er_3Ni_2 structure, whereas the corresponding Ln_3Pd_2 phases are unknown.

In Fig. 1 we have plotted the lattice parameters vs. the radii of the trivalent rare-earth ions (in 6-coordination) after Shannon [7]. The data of the Pd analogues are included for comparison. Surprisingly, the effects of Pd and Pt on *a* and *c* are opposite and this behaviour is reproduced in the actinides (see Table 2 and [2]). This appears to point to different wavefunctions of Pd and Pt. The size of these elements varies rather irregularly with their valence state. In the metallic state the Pd atom is almost 1% smaller than the Pt atom. For the divalent ions in square-planar coordination the relation is just the opposite (Pd^{2+}, 0.64 Å; Pt^{2+}, 0.60 Å), whereas in the tetravalent state in octahedral coordination palladium is again smaller (Pd^{4+}, 0.615 Å; Pt^{4+}, 0.625 Å) (radii from Shannon [7]).

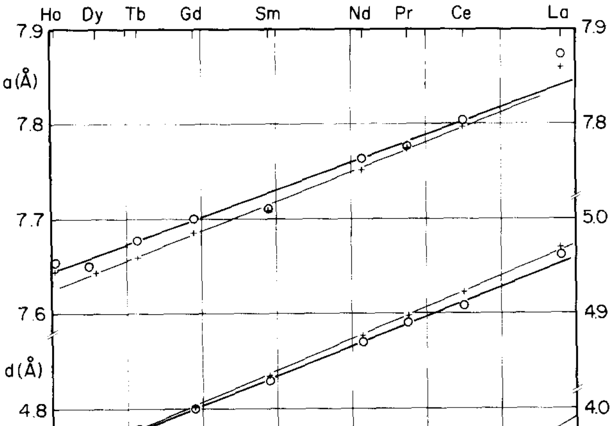

Fig. 1. The variation of *a*, *c* and $d = (V/Z)^{1/3}$ of the Ln_2Pt_2In compounds with the size of the rare-earth elements as compared with the corresponding data of the isostructural Ln_2Pd_2In compounds. *V*/*Z* is the volume per formula unit. The Ln^{3+} radii for coordination number six of Shannon [7] are used.

Table 2

Room temperature lattice parameters of the Mo_2FeB_2-type compounds Ln_2Pt_2In and Th_2Pt_2In; space group *P4/mbm* (no. 127), tP10; T=295 K. For comparison the data for U_2Pt_2In and Np_2Pt_2In [2] are added in italics. The standard deviations added in parentheses refer to the statistical error only; the additional error due to calibration and off-stoichiometry may be at least as large. The X-ray densities d_X are calculated based on the nominal compositions

Ln, *An*	*a* (Å)	*c* (Å)	*c*/*a*	*V* (Å³)	d_X (g cm⁻³)
La	7.8735(4)	3.9433(4)	0.50083(7)	244.45(4)	10.64
Ce	7.8038(3)	3.8830(2)	0.49758(5)	236.47(3)	11.03
Pr	7.7762(4)	3.8695(4)	0.49760(6)	233.99(5)	11.17
Nd	7.7639(3)	3.8331(3)	0.49371(5)	231.06(4)	11.41
Sm	7.7108(7)	3.7896(5)	0.49146(11)	225.32(8)	11.88
Gd	7.7009(7)	3.7348(6)	0.48498(11)	221.49(7)	12.29
Tb	7.6772(4)	3.7051(4)	0.48262(6)	218.38(5)	12.51
Dy	7.6511(6)	3.6767(5)	0.48055(10)	215.23(6)	12.81
Ho	7.6545(6)	3.6506(6)	0.47692(11)	213.89(7)	12.96
Y	7.6586(4)	3.6768(4)	0.48009(9)	215.66(5)	10.52
Th	7.659(2)	3.618(1)	0.4724(2)	212.2(1)	15.17
U [2]	*7.687(3)*	*3.701(4)*	*0.4815(8)*	*218.7(4)*	*14.90*
Np [2]	*7.6879(9)*	*3.7199(11)*	*0.4839(3)*	*219.9(2)*	*14.79*

The representation of the $r_{Ln}{}^{3+}$ dependence is rather sensitive to deviations that may occur for certain members. Thus, we deduce from Fig. 1 that Ce in Ce_2Pt_2In is fairly close to trivalent, which is corroborated by magnetic measurements. However, down to 1.5 K our Ce_2Pt_2In sample did not order magnetically and its susceptibility showed a strong influence of the crystal electric field. Pr_2Pt_2In was found to be ferromagnetic below T_C = 9.5 K. Our polycrystalline bulk sample was, at 1.6 K, saturated in a field of 4 kOe (2.2 μ_B in 4 kOe, 2.3 μ_B in 100 kOe). Nd_2Pt_2In has a higher Curie point: $T_C \approx 17$ K. Magnetization measurements at 1.7 K on two different parts of the same sample nicely demonstrated the influence of anisotropy (one sample: 1.2 μ_B in 5 kOe, linear to 1.7 μ_B in 100 kOe; the second sample: 2.1 μ_B in 4 kOe, linear to 2.3 μ_B in 100 kOe). Sm_2Pt_2In shows deviations in both lattice parameters *a* and *c* (Fig. 1), which may be due to Sm deficit. The closeness of the excited *J* state is responsible for the characteristic non-Curie–Weiss behaviour of $\chi(T)$, but a ferromagnetic impurity with $T_C \approx 28$ K falsified above all the low-temperature behaviour of our sample. Tb_2Pt_2In orders antiferromagnetically below T_N = 40 K, and above 80 K $\chi(T)$ obeys the Curie–Weiss law with an effective moment of 9.75 μ_B and θ_p = 33 K. At 2.4 K the magnetization curve revealed a distinct transition near 18 kOe, saturated above 40 kOe (5.2 μ_B in 100 kOe). Antiferromagnetic Ho_2Pt_2In (T_N = 8 K, p_{eff} = 10.3 μ_B, θ_p = 3 K) also undergoes a magnetic transition to a ferromagnetic order (at 2 K near 4 kOe; saturation moment of our sample at 100 kOe: 5 μ_B). Although these preliminary measurements were carried out on impurity-containing polycrystalline samples (so that the saturation moments represent averages between the easy-axis and the hard-axis values) they nevertheless can provide some first coarse information on the magnetic behaviour of these phases.

Acknowledgements

The author thanks Mr Stefan Siegrist for technical assistance, Dr Oscar Vogt for the permission to use his moving-sample magnetometer, and last but not least, Professor H.C. Siegmann as well as the Swiss National Science Foundation for continuous support.

References

[1] F. Hulliger and B. Xue, *J. Alloys Comp.*, (1994) in press.

[2] M.N. Peron, Y. Kergadallan, J. Rebizant, D. Meyer, J.M. Winand, S. Zwirner, L. Havela, H. Nakotte, J.C. Spirlet, G.M. Kalvius, E. Colineau, J.L. Oddou, C. Jeandey and J.P. Sanchez, *J. Alloys Comp., 201* (1993) 203.

[3] P. Villars and L.D. Calvert, *Pearson's Handbook of Crystallographic Data for Intermetallic Phases*, 2nd edn., American Society for Materials, Materials Park, OH, 1991.

[4] G. Steinberg and H.U. Schuster, *Z. Naturforsch. B, 34* (1979) 1237.

[5] F. Mirambet, P. Gravereau, B. Chevalier, L. Trut and L. Etourneau, *J. Alloys Comp., 191* (1993) L1.

[6] K. Yvon, W. Jeitschko and E. Parthé, *J. Appl. Crystallogr., 10* (1977) 73.

[7] R.D. Shannon, *Acta Crystallogr., A 32* (1976) 751.